3

Externally and Internally Pivoted Shoe Brakes

Typical externally and internally pivoted shoe brakes are shown in Figures 1 and 2. In all but extremely rare designs, equal forces act upon both shoes to produce equal applied moments about their pivots. External shoe brake control is usually through a lever system that may be driven by electro-mechanical, pneumatic, or hydraulic means. Internal shoe brake control is usually by means of a double-ended cylinder or a symmetrical cam.

Calculation of the moments and shoe lengths to achieve a specified braking torque cannot be carried out directly when the two shoes are pivoted as shown in either of these figures and when the opposing shoes are subjected to equal moments. The tedious task of manually iterating these formulas to get a satisfactory design under these conditions may be eliminated with the use of computer programs, such as those mentioned in the following sections, that can quickly produce either graphical or numerical design solutions.

I. PIVOTED EXTERNAL DRUM BRAKES

A. Long Shoe Brakes

Externally pivoted, long shoe brakes similar to that shown in Figure 1 are often used as holding brakes. As its name implies, a holding brake is to hold a shaft stationary until the brake is released. The compression spring on the left-hand side of the brake in Figure 1 applies a clamping force to the brake shoes

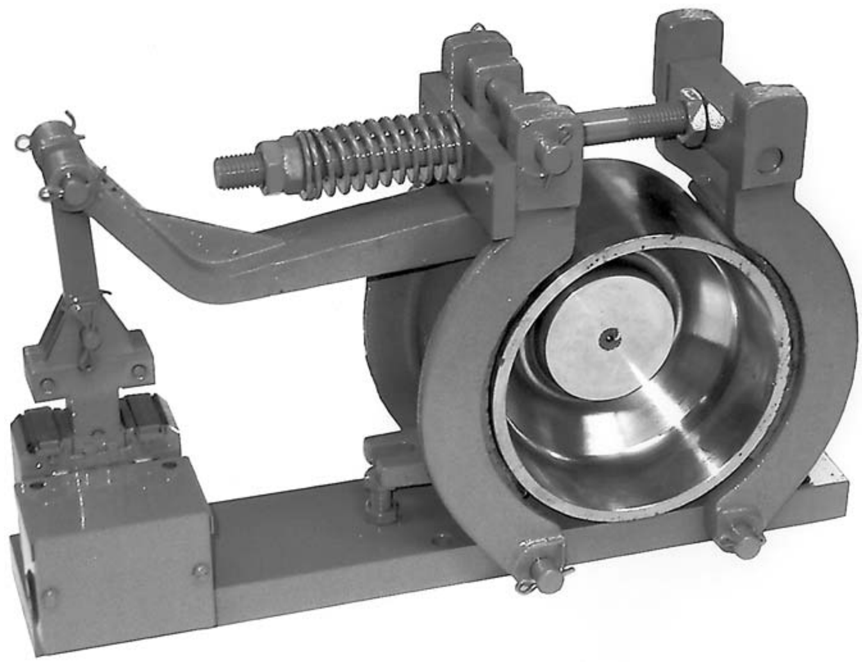

FIGURE 1 Externally pivoted shoe brake. (Courtesy Automation & Process Technology Div., Ametek Paoli, PA.)

on either side of the brake drum to hold it stationary without the need for external power. Electrical current through the solenoid on the left side of the assembly releases the brake and holds it open for as long as voltage is applied to the solenoid. Other holding brakes may use slightly different mechanical arrangements and may use either a hydraulic or a pneumatic cylinder to release the brake.

One of the applications of a holding brake is in the design of an overhead crane. The value of a holding brake is that it allows a load that has been raised to be held in position without external power. This is also a safety feature because the crane will not allow its load to be raised or lowered until the brake is intentionally released. Likewise, these brakes are also used in hoists, in punch and forming presses, and in some conveyor systems, for similar reasons.

We begin the derivation of the governing equations for the braking torque by considering only one shoe (Figure 3) and then extending those results to more than one shoe. Under the assumption that the shoe, lever, and drum are all rigid, and that the stress–strain relations of the lining are linear,

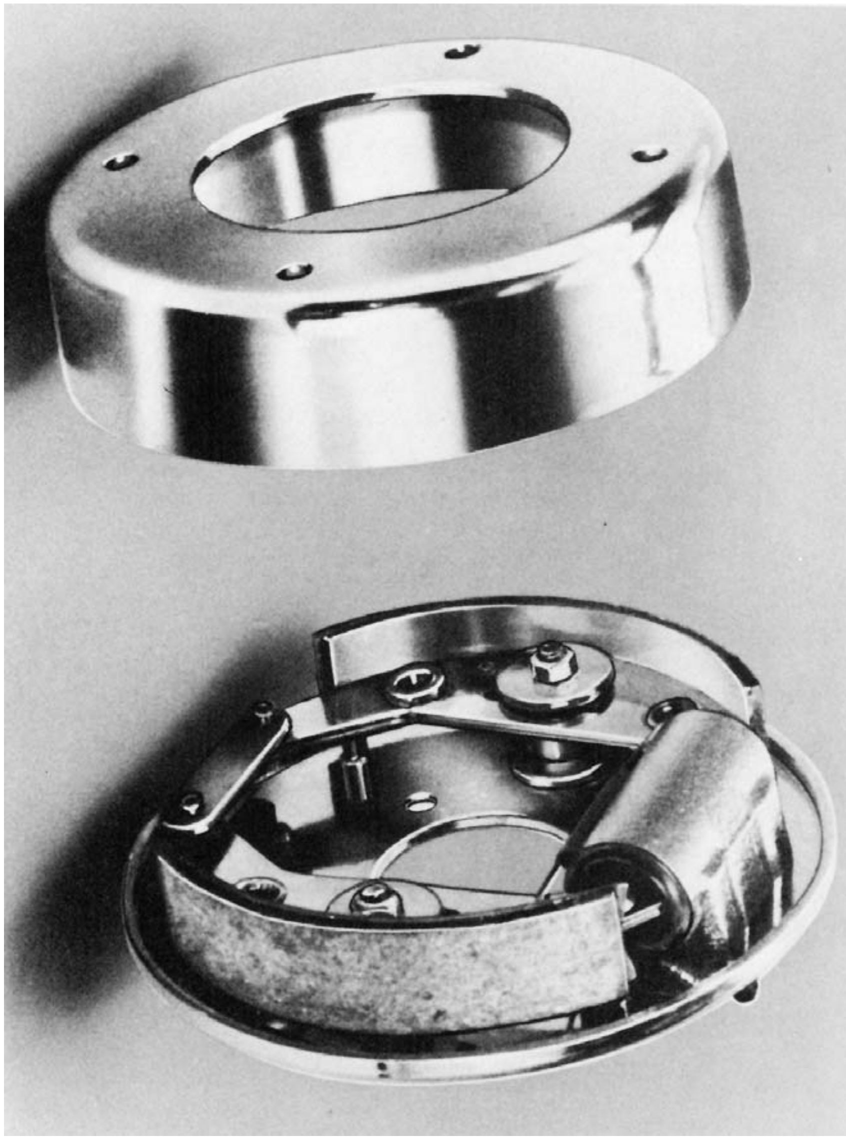

Figure 2 Internal pivoted shoe brake. (Courtesy of Dyneer Mercury Products, Canton, Ohio.)

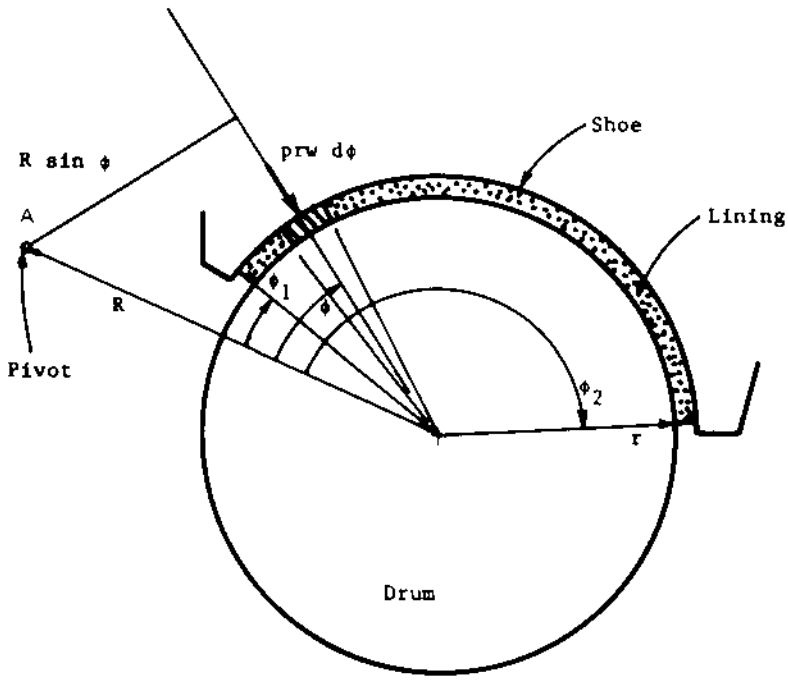

FIGURE 3 Geometry involved in calculating moment M_p about pivot point A.

the pressure p at any position along the lining due to infinitesimal rotation $\delta\beta$ of the shoe about pivot A will be given by

$$p = kR\delta\beta \sin\varphi \tag{1-1}$$

in terms of the quantities shown in Figure 3. Upon the introduction of the maximum pressure, written as

$$p_{\max} = kR\delta\beta\ (\sin\phi)_{\max} \tag{1-2}$$

we find that

$$kR\delta\beta = \frac{p_{\max}}{(\sin\phi)_{\max}} \tag{1-3}$$

so that after substitution from equation (1-3) into equation (1-1), we find that the pressure may be written in terms of the maximum pressure as

$$p = \frac{p_{\max}}{(\sin\phi)_{\max}} \sin\phi \tag{1-4}$$

With this expression for pressure as a function of position, the torque on the drum will be the integral over the shoe length of the incremental friction force $\mu(prw - d\phi)$ acting on the surface of a drum of radius r. Thus

$$T = \mu r^2 w \frac{p_{\max}}{(\sin\phi)_{\max}} \int_{\phi_1}^{\phi_2} \sin\phi \; d\phi \tag{1-5}$$

in which $(\sin\phi)_{\max}$ denotes the maximum value of $\sin\phi$ within the range $\phi_1 \le \phi \le \phi_2$. Integration of equation (1-5) yields

$$T = \frac{\mu p_{\max} r^2 w}{(\sin\phi)_{\max}} (\cos\phi_1 - \cos\phi_2) \tag{1-6}$$

in which ϕ_1 is the angle from radius R between the drum axis and pivot A to the near edge of the drum sector subtended by the brake lining. As drawn in Figure 3, angle ϕ_2 is measured from radius R toward the far edge of the brake lining. Hence the angle subtended by the shoe is given by

$$\phi_0 = \phi_2 - \phi_1 \tag{1-7}$$

To calculate the moment that must be applied about pivot A in Figure 3 to obtain the torque found by equation (1-6), we first calculate the moment reaction at the pivot due to both the incremental normal forces and the incremental friction forces acting on the lining. An equal and opposite moment must, of course, be supplied to activate the brake.

Radial force $prw\; d\phi$ on each incremental area also contributes to a pressure moment M_p about pivot A. Relative to the geometry in Figure 3, and with the aid of equation (1-4), this moment may be written as

$$M_p = \int_{\phi_2}^{\phi_2} (pwr\; d\phi) R \sin\phi = \frac{p_{\max}\, wrR}{(\sin\phi)_{\max}} \int_{\phi_1}^{\phi_2} \sin^2\phi \; d\phi \tag{1-8}$$

which integrates to

$$M_p = \frac{p_{\max}\, wrR}{4(\sin\phi)_{\max}} (2\phi_0 - \sin 2\phi_2 + \sin 2\phi_1) \tag{1-9}$$

where ϕ_0 is given by equation (1-7). This moment is positive in the counter-clockwise direction, and its algebraic sign is independent of the direction of drum rotation relative to the brake lever's pivot point.

Reactive moment M_f at pivot A due to the friction force acting on the shoe may be calculated using the geometry sketched in Figure 4. Thus,

$$\begin{aligned} M_f &= \int_{\phi_1}^{\phi_2} (\mu pwr\; d\phi)(R\cos\phi - r) \\ &= \frac{\mu p_{\max}\, wr}{(\sin\phi)_{\max}} \int_{\phi_1}^{\phi_2} (R\cos\phi \sin\phi - r\sin\phi) d\phi \end{aligned} \tag{1-10}$$

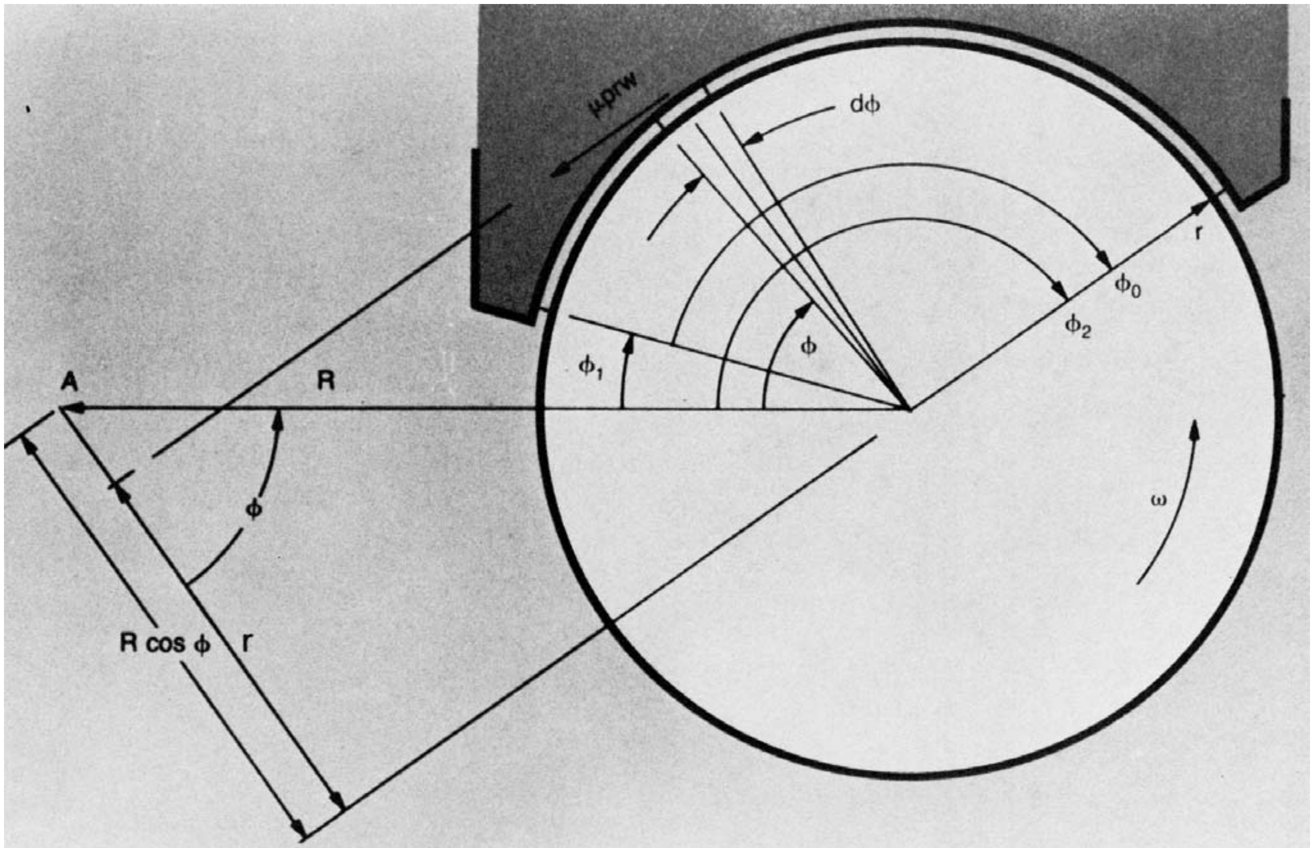

FIGURE 4 Geometry involved in calculating moment M_f about pivot point A.

Integration of equation (1-10) yields

$$M_f = \frac{\mu p_{\max} wr}{4(\sin \phi)_{\max}}[R(\cos 2\phi_1 - \cos 2\phi_2) - 4r(\cos \phi_1 - \cos \phi_2)] \quad (1\text{-}11)$$

Here the quantity enclosed by the square brackets determines the algebraic sign of M_f and may cause it to be zero. The physical significance of the algebraic sign for nonzero values of moment M_f depends upon the direction of rotation ω of the drum.

If the rotation is toward the pivot, as in Figure 4, a positive value of M_f signifies a clockwise moment about the pivot that applies the brake by forcing the shoe against the drum, which would cause self-locking. Therefore, a negative or zero value for M_f from equation (1-11) is required to produce either a counterclockwise or a zero moment, respectively, about the pivot point.

The interpretation is reversed if the drum rotation ω is away from the pivot. In this case a positive value from equation (3.11) indicates a counterclockwise rotation of the shoe about the pivot that tends to release the brake. Obviously, a negative value in this situation indicates a clockwise moment about the pivot that tends to rotate the shoe toward the drum.

From these observations it follows that brake activation requires an applied moment M_e about the pivot point A such that

$$\begin{aligned} M_p + M_f = M_e > 0 &\qquad \omega \text{ away from the pivot} \\ M_p - M_f = M_e > 0 &\qquad \omega \text{ toward the pivot} \end{aligned} \quad (1\text{-}12)$$

where M_f itself, as calculated from equation (1-11), must be negative or zero when rotation ω is toward the pivot and positive or zero when it is away from the pivot—hence the minus sign in the second of equations (1-12).

Self-locking is of use only when the brake is to serve as a backstop or as an emergency brake during control failure. Otherwise, self-locking is generally to be avoided because it does not allow the braking torque to be controlled by the control of M_e.

B. Short Shoe Brakes

Short shoe brakes are generally defined as those for which the angular dimension of the brake, ϕ_0, is small enough (generally less than 20°) that $\sin \phi \cong (\sin \phi)_{\max}$ and $p \cong p_{\max}$ so that with these restrictions equation (1-5) may be approximated by

$$T = \mu p w r^2 \phi_0 = \mu r F \quad (1\text{-}13)$$

where

$$F = p w r \phi_0 \quad (1\text{-}14)$$

is the force exerted on the short shoe. Application of these approximations to equation (1-9) before integration yields

$$M_f = \mu F(R \cos \phi_1 - r) \tag{1-15}$$

Similarly, application of these approximations to equation (1-10) before integration yields

$$M_p = FR \sin \phi_1 \tag{1-16}$$

so that substitution into equation (1-12) with the minus sign in effect reveals that the short shoe will not be self-locking if

$$\sin \phi_1 - \mu\left(\cos \phi_1 - \frac{r}{R}\right) > 0 \tag{1-17}$$

II. PIVOTED INTERNAL DRUM BRAKES

The equations derived in Section IA dealing with long external shoe brakes apply equally well to internal shoe drum brakes. There is one essential difference, however, that does not appear explicitly in the equations themselves: The physical significance of positive values of moments M_p and M_f is different. The geometry used to obtain these relations for internal shoe brakes is shown in Figures 5 and 6; the different interpretations for the various combinations of direction of rotation and internal or external shoes are listed in Table 1. In that table rotation of the drum from the far end of the shoes to the end near the pivot (termed rotation from the toe of the brake to the heel) is indicated by an arrow pointing toward the letter p; rotation in the opposite direction is indicated by an arrow pointing away from the letter p. The acronym cw indicates clockwise rotation (or the direction of rotation of an advancing right-hand screw), and ccw indicates counter-clockwise rotation.

From Figure 5 it follows that

$$dM_f = (\mu wrp \, d\phi)(r - R \cos \phi) \tag{2-1}$$

This is the negative of the integrand in equation (1-10). The rotation indicated causes the shoe to pivot in the counterclockwise direction about A; but because equation (1-10) used the negative of the integrand above, the rotation shown corresponds to a negative M_f value as calculated using either equation (1-10) or equation (1-11). Hence, negative M_f from these formulas implies counterclockwise rotation and positive M_f corresponds to clockwise rotation of the shoe about its pivot.

Braking requires a moment M_a applied to the shoe as given by

$$M_p - M_f = M_a \qquad \omega \text{ away from the pivot}$$

$$M_p + M_f = M_a \qquad \omega \text{ toward the pivot}$$

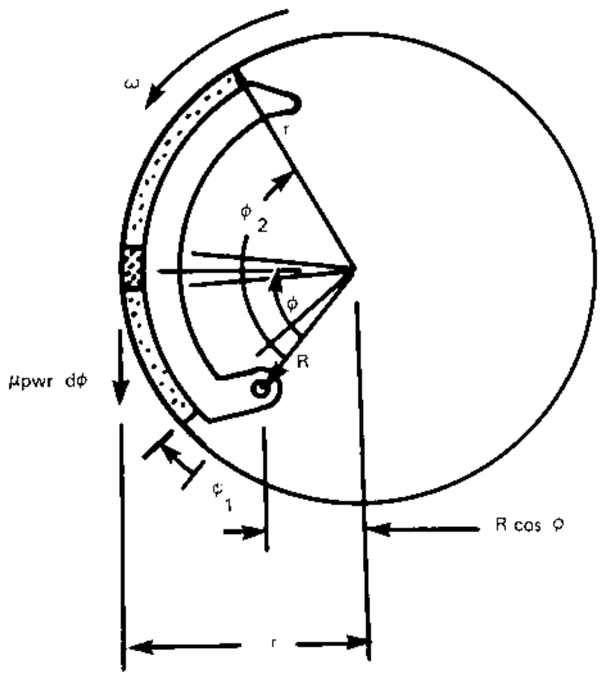

FIGURE 5 Geometry for calculating the moment due to friction about point *A* for an internal shoe brake.

for internal shoes. The physical significance of the algebraic signs associated with the moment expressions derived in the preceding sections as applied to external and internal brakes is displayed in Table 1. It is may be helpful the rewrite the equations for either internal or external brakes in terms of different symbols if the use of a single set of equations for two different cases becomes too confusing. After using these equations enough to become familiar with them, the reader may find that analysis is easier if they are again combined into a single set, as has been done here.

Drum brake efficiency may be measured in terms of the ratio of the torque produced by the brake itself to the torque required to activate the brake, also known as the shoe factor; namely,

$$\frac{T}{M_a} = \frac{T}{M_p \pm M_f} \tag{2-2}$$

Brake efficiency is generally not a design factor in the analysis of drum brakes because it is dependent on too many factors [ϕ_1, ϕ_2, r/R, μ, w, and $(\sin\phi)_{\max}$]

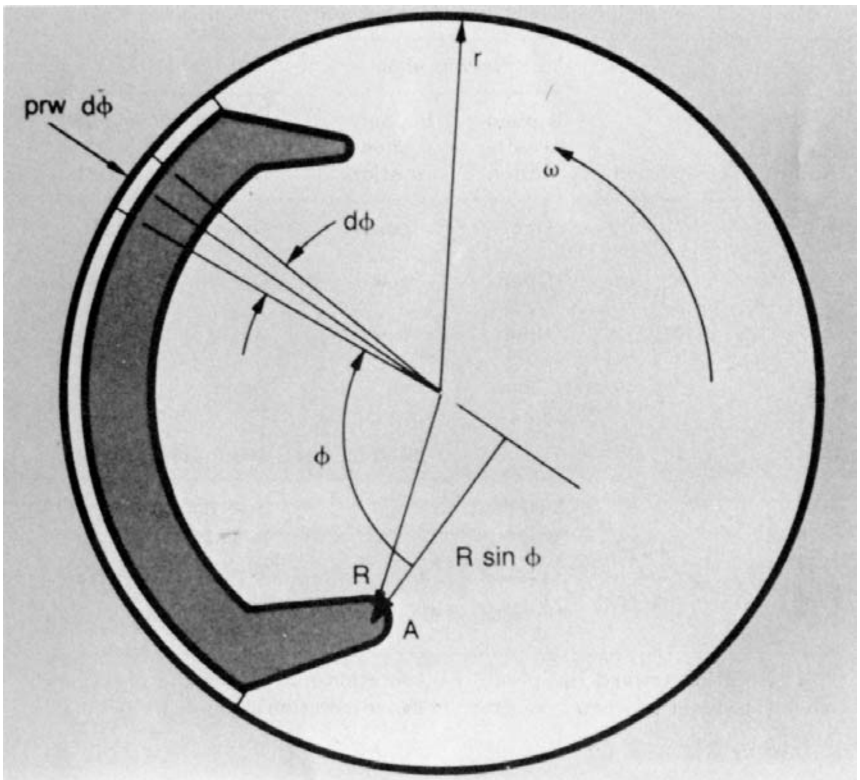

FIGURE 6 Geometry for calculating the moment due to pressure about point *A* for an internal shoe brake.

to make it useful. More significance is usually associated with brake life, heat dissipation, fading, and braking torque capability.

III. DESIGN OF DUAL-ANCHOR TWIN-SHOE DRUM BRAKES

For both external and internal shoes and for either direction of rotation a positive M_e value indicates that an external moment of that magnitude must be applied to activate the brake. The formulas also clearly indicate that the extent of the braking action may be controlled by controlling this activation moment. The role of M_f, the moment due to friction, in determining the required activation moment M_e may be seen by returning to equation (1-11)

TABLE 1 Moment Relations for Internal and External Drum Brakes

		External shoe		Internal shoe	
Rotation[a]	Moment	Implied braking action	Implied shoe rotation	Implied braking action	Implied shoe rotation
$p\rightarrow$	$M_p > 0$	Open	ccw	Open	cw
$p\leftarrow$	$M_p > 0$	Open	ccw	Open	cw
$p\rightarrow$	$M_f > 0$	Open	ccw	Close	ccw
$p\leftarrow$	$M_f > 0$	Close	cw	Open	cw
		Applied Moment Relations			
		External Shoe		Internal Shoe	
$p\rightarrow$	–	$M_p + M_f = M_a$		$M_p - M_f = M_a$	
$p\leftarrow$	–	$M_p - M_f = M_a$		$M_p + M_f = M_a$	

[a] $p\rightarrow$, Rotation toward the pivot; $p\leftarrow$, rotation away from the pivot; cw, clockwise rotation; ccw, counterclockwise rotation.

and observing that this moment may be either positive or negative, depending on the choices for the quantities appearing in brackets.

One measure of the contribution of the friction moment to the entire amount acting to force the shoe against the drum is the actuation factor, defined by

$$\frac{M_f}{M_a} \qquad \left(\text{sometimes defined as } \frac{M_f}{M_p}\right) \tag{3-1}$$

which is independent of the torque produced by the brake.

If the quantities in brackets in equation (1-11) are chosen such that the bracket becomes both negative and relatively large, M_f may dominate M_p and M_a becomes negatfive. This means that the brake has become self-locking: contact between the shoe and the drum causes uncontrolled motion of the shoe toward the drum. Since the resulting braking action is beyond the control of the usual single-direction activation mechanism, self-locking is generally to be avoided.

Return to relations (2-2), equate the denominators, and then divide both sides by M_p, which is always positive, to obtain

$$\frac{M_a}{M_p} = 1 \pm \frac{M_f}{M_p} \tag{3-2}$$

Hence self-locking of external brakes in which the drum rotates toward the pivot can be avoided if the relation M_f/M_p is always less than $+1$; if the drum rotates away from the pivot, self-locking can be avoided if M_f/M_p is always greater than -1. Similar criteria hold for internal brakes except that the directions of rotation are reversed for the same algebraic signs. Since most brakes are designed for rotation in both directions, it is generally convenient to combine these criteria into a single criterion, which is that self-locking of both internal and external drum brakes may be avoided if

$$-1 \leq \frac{M_f}{M_p} \leq +1 \tag{3-3}$$

Selection of shoe and drum angles and dimensions in accordance with this criterion may be aided by construction of design curves such as illustrated in Figures 7 and 8, in which the ratio $M_f/\mu M_p$ is plotted against angle ϕ_2 for selected values of the coefficient of friction. External shoes are characterized by R/r ratios greater than unity and internal shoes by r/R ratios less than unity. The ratio $M_f/\mu M_p$ has been plotted instead of M_f/M_p in Figures 7 and 8 because it itself is independent of the coefficient of friction and thus must be

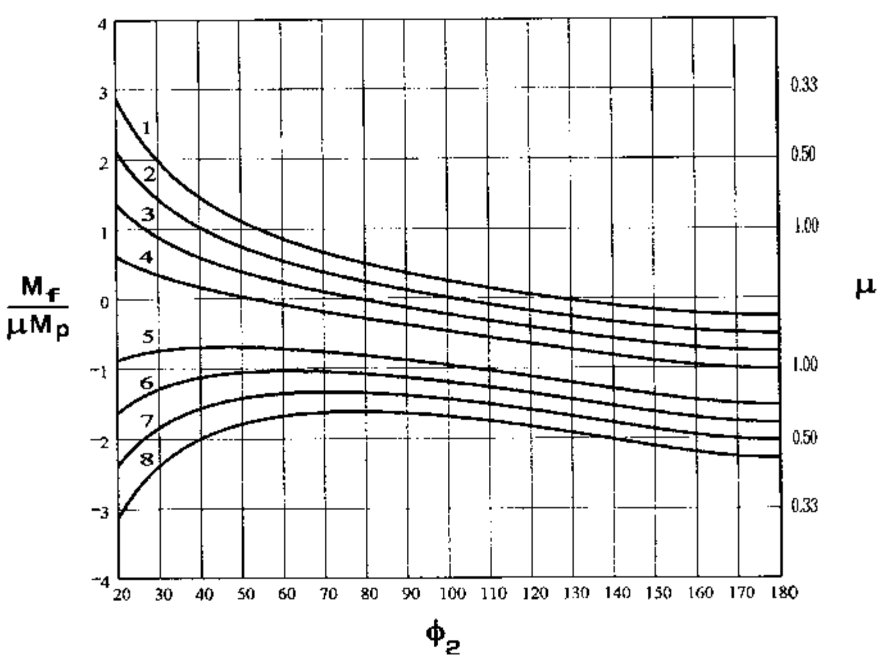

FIGURE 7 Design curves for $M_f/(\mu M_p)$ for $\varphi_1 = 10°$. r/R ratios for the upper, external brake, curves are: 1—$r/R = 0.2$; 2—$r/R = 0.4$; 3—$r/R = 0.6$; 4—$r/R = 0.8$. r/R ratios for the lower, internal brake, curves are: 5—$r/R = 1.2$; 6—$r/R = 1.4$; 7—$r/R = 1.6$; 8—$r/R = 1.8$.

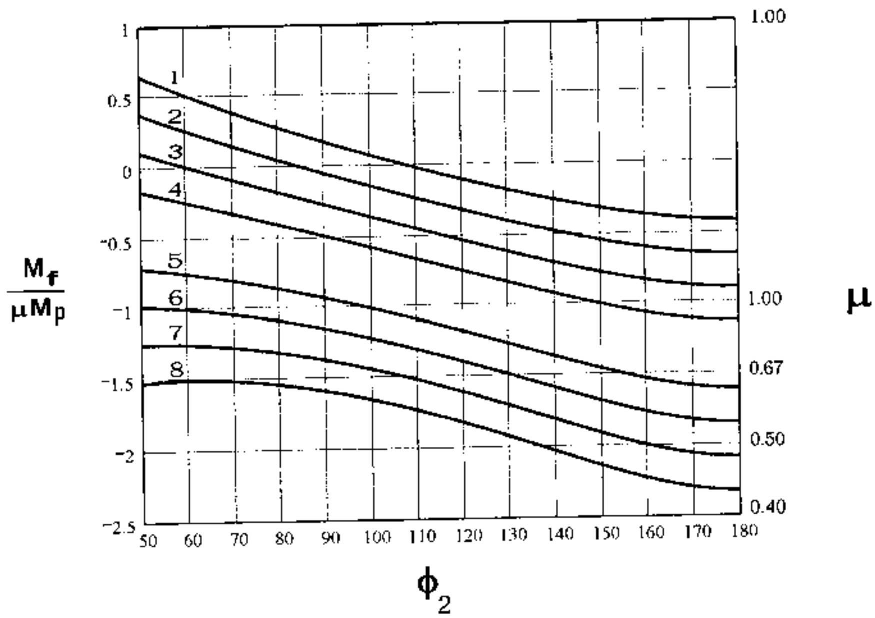

FIGURE 8 Design curves for $M_f/(\mu M_p)$ for $\varphi_1 = 45°$. *r/R* ratios for the upper, external brake, curves are: 1—*r/R* = 0.2; 2—*r/R* = 0.4; 3—*r/R* = 0.6; 4—*r/R* = 0.8. *r/R* ratios for the lower, internal brake, curves are: 5—*r/R* = 1.2; 6—*r/R* = 1.4; 7—*r/R* = 1.6; 8—*r/R* = 1.8.

plotted only once. To use it for any coefficient of friction within the range shown, it is only necessary to note that the requirement that the ratio M_f/M_p lie between -1 and $+1$ is equivalent to

$$-\frac{1}{\mu} \leq \frac{M_f}{\mu M_p} \leq \frac{1}{\mu} \tag{3-4}$$

Since $p_{\max}$, $(\sin\phi)_{\max}$, and μ cancel out when equation (1-11) is divided by the product of μ and equation (1-9), the ratio $M_f/(\mu M_p)$ is a function of only three quantities: r/R, ϕ_1, and ϕ_2. Thus, $M_p/(\mu M_p)$ may be plotted as a function of ϕ_2 for fixed values of r/R and ϕ_1, as in Figures 7 and 8. Criterion (3.4) also can be included in these graphs by noting that $1/\mu > 0$ pertains to external drum brakes and $1/\mu < 0$ pertains to internal drum brakes, so these values may be shown on the left-hand ordinate of these graphs by relating them to the limiting values of $M_f/(\mu M_p)$ according to relation (3.4), namely, that at the lower limit,

$$-1/\mu = M_f/(\mu M_p)$$

and that at the upper limit,

$$1/\mu = M_f/(\mu M_p)$$

Consequently, the ordinates on the right-hand sides of the graphs in Figures 7 and 8 are the reciprocals of the ordinates on the left-hand sides. Thus, we may read directly from these graphs that to be non-self-locking, the $M_f/(\mu M_p)$ ratio must fall below the $1/\mu$ value for external drum brakes, and it must fall above the $-1/\mu$ value for internal drum brakes.

Note that these curves show that the range of possible values for $M_p/(\mu M_p)$ that ensure that a dual-shoe brake will be free of self-locking decreases as the lining coefficient of friction increases, as should be expected.

The length of a single shoe for a desired torque may be found algebraically from equation (1-6). However, selection of the shoe length to provide a specified braking torque cannot be accomplished directly if two external or two internal shoes operating about fixed pivot points, or anchor pins, are to be used for greater braking torque.

Whenever two shoes are required and the arc length of the lining, $r\phi_0 = r(\phi_2 - \phi_1)$, is to be selected, it is necessary to select ϕ_1, say, and then find a value of ϕ_2 such that the total torque T is the sum of T_a and T_b, where T_a represents the braking torque contribution from the shoe with the larger peak pressure and T_b represents the braking torque from the shoe with the smaller peak pressure, p_b. Torque T_a, as given by the equation

$$T_a = \frac{\mu p_a r^2 w}{(\sin \phi)_{\max}}(\cos \phi_1 - \cos \phi_2) \tag{3-5}$$

will be the reference torque for both shoes. For simplicity in writing the remaining equations it is convenient to introduce the quantities

$$\begin{aligned} A &= R(2\phi_2 - 2\phi_1 - \sin 2\phi_2 + \sin 2\phi_1) \\ B &= \mu[R(\cos 2\phi_1 - \cos 2\phi_2) - 4r(\cos \phi_1 - \cos \phi_2)] \\ b_a &= p_a b \qquad b_b = p_b b \qquad b = \frac{rw}{4(\sin \phi)_{\max}} \end{aligned} \tag{3-6}$$

so that moments M_f and M_p may be written as

$$\begin{aligned} M_{p_a} &= b_a A \qquad M_{f_a} = b_a B \\ M_{p_b} &= b_b A \qquad M_{f_b} = b_b B \end{aligned} \tag{3-7}$$

In these terms the applied moment to one of the shoes may be written as

$$M_a = b_a \min \begin{cases} (A + B) \\ (A - B) \end{cases} \tag{3-8}$$

and the relation

$$M_a = b_b \max \begin{cases} (A + B) \\ (A - B) \end{cases} \tag{3-9}$$

then determines the maximum pressure on the other shoe. Recall that braking torque T is linearly dependent on the maximum pressure, in this case p_a, so

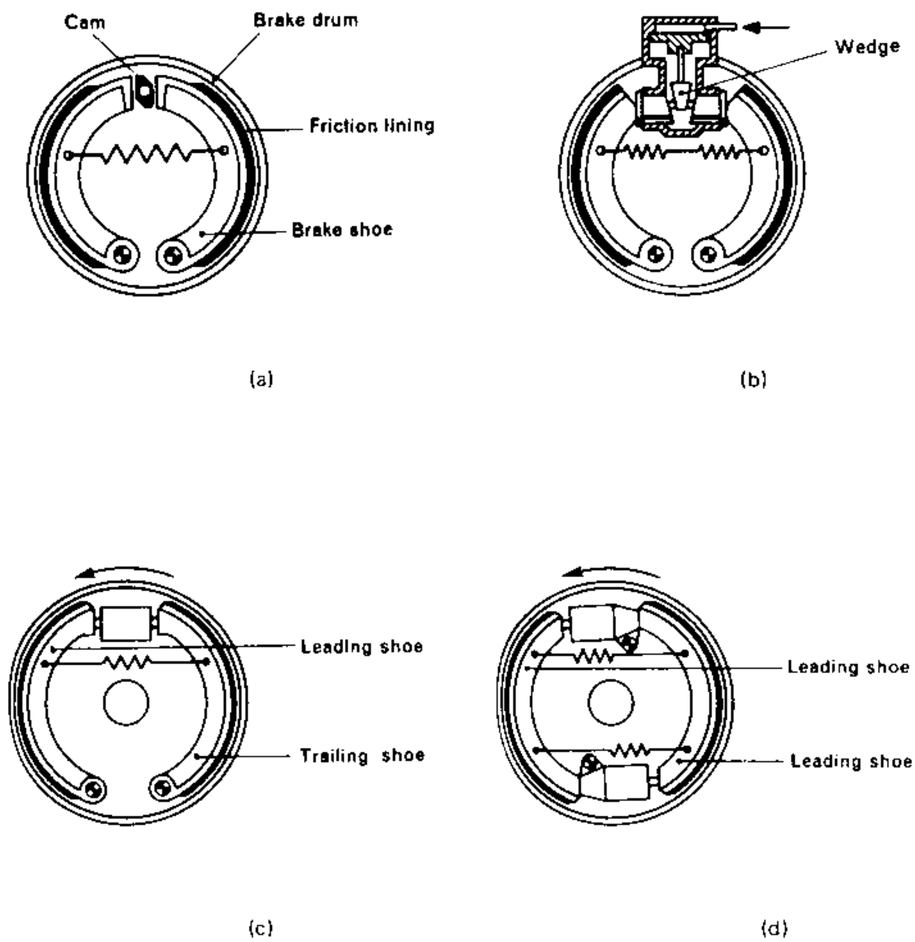

FIGURE 9 Four styles of dual-anchor brakes: (a) cam brake; (b) wedge brake; (c) simplex brake; (d) duplex brake.

that reevaluation of the integral in equation (1-5) is not necessary whenever the two shoes are of the same size; T_b is simply given by

$$T_b = \frac{p_b}{p_a} T_a = \frac{b_b}{b_a} T_a \tag{3-10}$$

Consequently, the total braking torque expression becomes

$$T = \left(1 + \frac{b_b}{b_a}\right) T_a \tag{3-11}$$

Designing a double-shoe brake, either internally pivoted (automotive type) or externally pivoted, to provide a specified braking torque consists of finding values that satisfy equations (2.2) and (3.5) through (3.11).

Moment M_a is most commonly applied by forces supplied by a cam at the toe of each brake, as shown in Figure 9(a), which is known as a cam brake; by an integral hydraulic system that drives a wedge between two pistons, which in turn act against the toe of each shoe, as shown in Figure 9(b), which is known as a wedge brake; or by a hydraulic cylinder between the two shoes, as shown in Figure 9(c), which is known as a simplex brake. In all of these the force necessary to provide moment M_a is given by

$$F = \frac{M_a}{2r \sin(\phi_0/2)} \tag{3-12}$$

The iteration process may be eliminated using the duplex brake shown in Figure 9(d), but at the expense of a brake that is more effective for one direction of rotation (rotation from toe to heel) than for the reverse rotation. This brake style is therefore usually limited to machines where rotation is in one direction, such as conveyor belts.

IV. DUAL-ANCHOR TWIN-SHOE DRUM BRAKE DESIGN EXAMPLES

Example 4.1

Design an external dual-anchor twin-shoe drum brake to provide a torque of 6050 N-m. The drum diameter should not exceed 400 mm and the drum thickness should not exceed 90 mm, based on interference with other machine components. If possible, select angle ϕ_1 to be 25° in order to use stock hydraulic components already under contract for other products. Heating during braking may occasionally be large.

Comparison of Figures 7 and 8 shows that increasing ϕ_1 from 10° to 45° has relatively little effect on these curves, so that we may refer to Figure 7 for $\phi_1 = 25°$. Hence we find that an external brake will be free of self-locking as long as the brake shoes subtend an angle of 70° or more.

Guided by the design limitations in the problem statement, let the drum diameter be 350 mm and the width be 80 mm to ensure extra clearance if needed. Both dimensions can be increased if no satisfactory brake can be designed within these smaller dimensions. Since we plan to design shoes having ϕ_2 of the order of 140° use this as an initial value of ϕ_2 along with $p_{max} = 3.00$ MPa (435 MPa), which may be had using a proprietary material from Chapter 1 that has $\mu_{bot} = 0.40$. Take $\mu = 0.35$ to find if this will yield a satisfactory shoe. If it does, the longer band will aid in cooling and may have a longer life The required activation moment M_a may be found from equation (3.9) after A and B have been calculated.

Upon entering the selected values

$T = 6,050,000$ N–m $\qquad R = 230$ mm

$w = 80$ mm $\qquad r = 175$ mm

$\mu = 0.35 \qquad \phi_1 = 25°$

$p_{max} = 3.00$ MPa

into a Mathcad work page as shown later we can use the graphics capability of Mathcad to produce the graph in Figure 10 to show the torque as a function of angle φ.

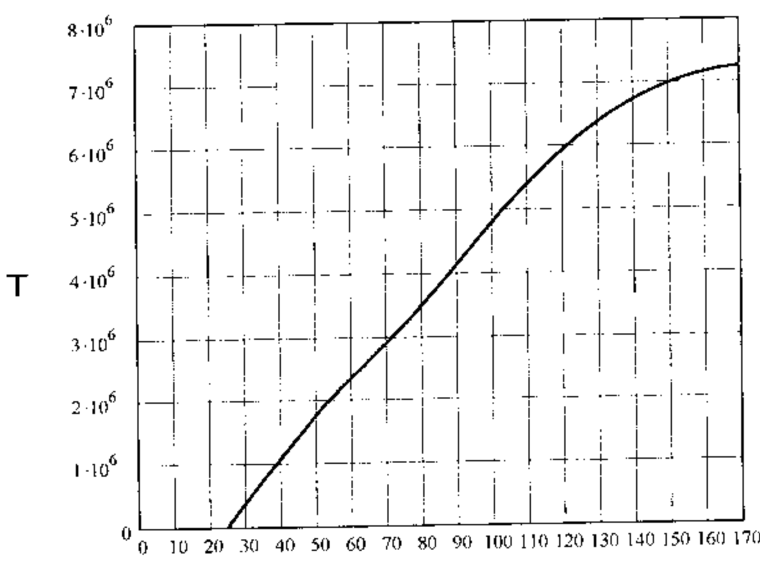

FIGURE 10 Torque vs. φ for an external drum brake.

The functional notation $\phi \cdot \deg$ in the trigonometric functions is a Mathcad requirement when ϕ is in degrees. It enters the corresponding radian measure as the argument of the trigonometric function involved.

No value for M_a is given because examination of equations (3.6) and (3.10) reveals that the torque is independent of M_a. It is dependent upon $p_{\max}$, the maximum pressure, which provides the activating forces.

$$w = 80 \qquad \mu = 0.35 \qquad R = 230 \qquad r = 175 \qquad \phi_1 = 25$$

$$p_{\max} = 3.00 \qquad T_0 = 605000$$

$$A(\phi) = R(2\phi \cdot \deg - 2\phi_1 \cdot \deg - \sin(2\phi \cdot \deg) + \sin(2\phi_1 \cdot \deg))$$

$$B(\phi) = \mu[R(\cos(2\phi \cdot \deg) - \cos(2\phi \cdot \deg)) - 4r(\cos(\phi_1 \cdot \deg) \\ - \cos(\phi \cdot \deg))]$$

$$C(\phi) = A(\phi) + B(\phi) \qquad D(\phi) = A(\phi) - B(\phi)$$

$$M_1(\phi) = \begin{cases} C(\phi) & \text{if } C(\phi) \leq D(\phi) \\ D(\phi) & \text{otherwise} \end{cases}$$

$$M_2(\phi) = \begin{cases} C(\phi) & \text{if } C(\phi) \geq D(\phi) \\ D(\phi) & \text{otherwise} \end{cases}$$

$$b_a(\phi) = \frac{1}{M_1(\phi)} \qquad b_b(\phi) = \frac{1}{M_2(\phi)}$$

$$\sin \phi_m(\phi) = \begin{cases} 1 & \text{if } \phi \geq 90 \\ \sin(\phi \cdot \deg) & \text{otherwise} \end{cases}$$

$$T_a(\phi) = \frac{(\mu p_{\max} r^2 w)}{\sin \phi_m(\phi)}(\cos(\phi_1 \cdot \deg) - \cos(\phi \cdot \deg))$$

$$T(\phi) = \left(1 + \frac{b_b(\phi)}{b_a(\phi)}\right) T_a(\phi)$$

The Track feature in Mathcad prints the coordinates of the points where the screen crosshairs lie upon a curve. Smooth transition from point to point along a curve may not be possible, however, because of the difficulty of producing very small motion of the tracking ball on the mouse being used. Nevertheless, we can come sufficiently close to be within most manufacturing and design tolerances. In this example we can read from Figure 10 that

$$T = 6{,}044{,}200 \text{ N-m} \qquad \text{at } \phi_2 = 122.57^\circ$$

$$T = 6{,}052{,}200 \text{ N-m} \qquad \text{at } \phi_2 = 122.74^\circ$$

Alternatively, the bisection procedure provided by TK Solver, which is more accurate, yielded $\phi_2 = 122.693^\circ$.

Example 4.2

Design an internal twin-shoe drum brake to provide a braking torque of 5800 N-m with an outside diameter of 350 mm and a shoe width of 80 mm using a lining material with a friction coefficient of 0.35. Use $\phi_1 = 25°$ and let the pivot radius be 120 mm, if possible, because of heat sensors to be included within the drum.

Substitution of the following values into the previous worksheet and graphing the resulting $T(\phi)$ as a function of ϕ yields the graph shown in Figure 11.

$$w = 80 \text{ mm} \qquad R = 120 \text{ mm}$$
$$r = 175 \text{ mm} \qquad \mu = 0.35$$
$$\varphi = 25°$$

From it we read that a torque of 5,798,700 N-m requires $\phi_2 = 155.38°$ and that a torque of 5,801,000 corresponds to an angle $\phi_2 = 155.55°$. The bisection value found from the TK Solver program was $\phi_2 = 156.4749°$. They serve as a check upon one another because the same formulas must be entered into each program to get agreement of the order shown. As before, the values read from Figure 11 are sufficiently precise for many brake applications.

Notice in both Figures 10 and 11 that increasing angle φ beyond about 120° yields diminishing returns; the torque no longer increases nearly linearly relative to φ.

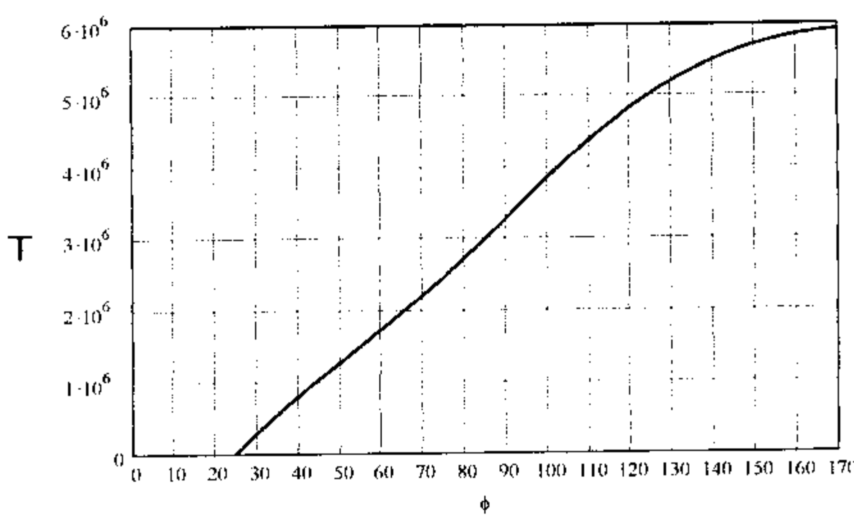

FIGURE 11 Torque vs. φ for in internal drum brake.

V. DESIGN OF SINGLE-ANCHOR TWIN-SHOE DRUM BRAKES

Internal shoe drum brakes of this type, as illustrated in Figure 12, which are also known as Bendix type, or servobrakes, have neither shoe permanently attached to an anchor pin. Each is free to shift position slightly as the direction of the drum reverses, so that for either direction of rotation one shoe pivots about the anchor pin and the othe other shoe pivots about its end of the adjusting link between shoes. Consequently, both shoes see rotation from toe to heel regardless of the direction of rotation. Although this construction facilitates the design of a self-adjusting mechanism for automotive use, it does not entirely eliminate the difference in wear between the two shoes, and it introduces additional labor to calculate brake torque and lining pressure. A

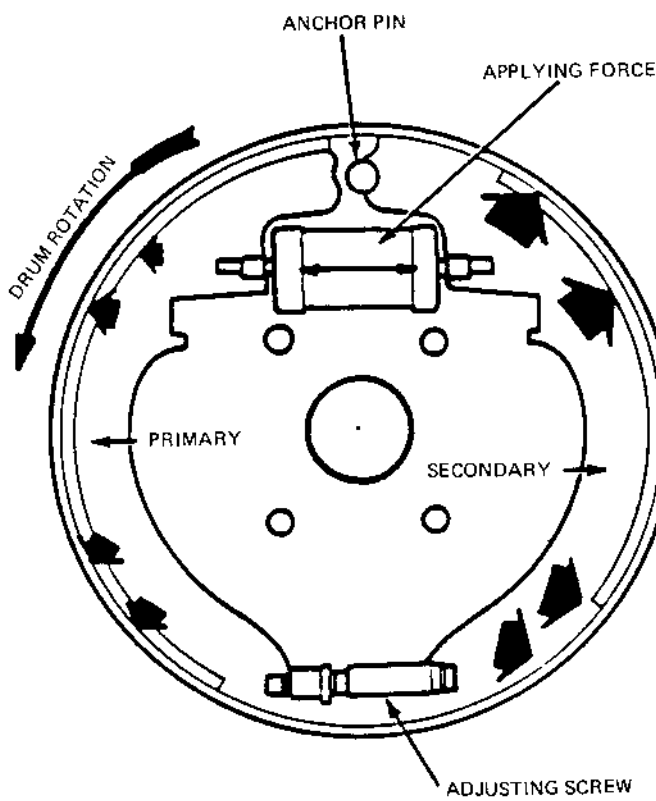

FIGURE 12 Schematic of a Bendix, or servo, single-anchor brake.

program to ease the latter tasks is described and demonstrated in the following paragraphs.

With this program it is easy to show that relatively small changes in the pressure distribution along either shoe may produce large changes in the braking torque.

Although calculation of the braking torque and consideration of the design of brakes of this type appears to be omitted from most of the machine design texts now in print, two of them do contain a brief narrative reference to their construction [1,2]. These brakes may be analyzed by the graphical method introduced by Fazekas [3] in 1957 or by the numerical method described in reference 4. In the first method the pressure is described only in terms of its center of pressure (due to the lack of easy computational facilities in 1957), while in the second method the pressure distribution is represented by either an approximating function or by a measured pressure distribution. The second method displays the marked effect the pressure distribution has on brake performance.

The governing equations for the primary shoe, which is the shoe not pivoted at the anchor pin (Figures 12 and 13), are the same as those given derived in Section 1, which are that the moments (positive in the clockwise

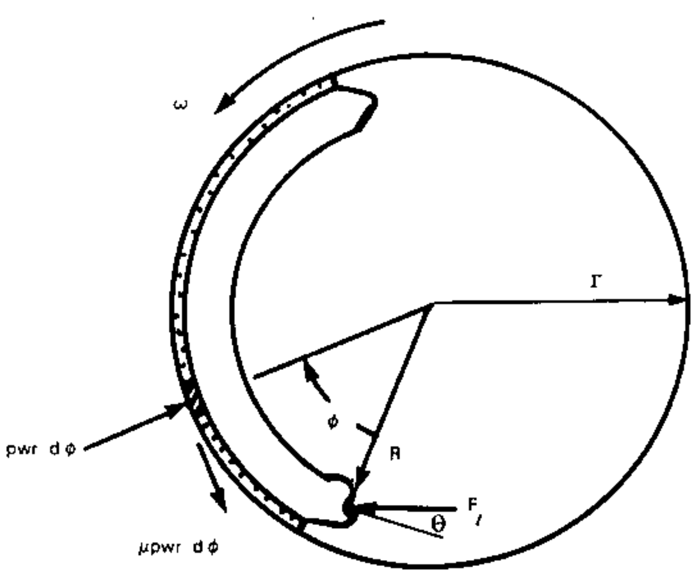

FIGURE 13 Primary link force and incremental pressure and friction forces.

direction) about the pivot due to the pressure and the frictional forces are given by

$$M_p = rwR\int_{\phi_1}^{\phi_2} p \sin\phi \; d\phi \tag{5-1}$$

and

$$M_f = \mu wr\int_{\phi_1}^{\phi_2} p(r - R\cos\phi)d\phi \tag{5-2}$$

which are repeated here for convenience. In the following discussion we shall need an expression for the radial and tangential force components acting on the pivot. These relations may be derived by taking components of the pressure and friction forces acting on the lining in directions parallel and perpendicular to R (Figure 13) from the center of the drum to the pivot point of the shoe. The result is that the force component in the radial direction is given by

$$F_{r_1} = -rw\int_{\phi_1}^{\phi_2} p\cos\phi \; d\phi + \mu rw\int_{\phi_1}^{\phi_2} p\sin\phi \; d\phi \tag{5-3}$$

and the force perpendicular to radius R is given by

$$F_{\theta_1} = rw\int_{\phi_1}^{\phi_2} p\sin\phi \; d\phi - \mu rw\int_{\phi_1}^{\phi_2} p\cos\phi \; d\phi \tag{5-4}$$

where θ is the angle between vector F_1 and a perpendicular to vector R.

Analysis based on these equations differs, however, from that associated with shoes having fixed pivot points. In particular, neither the sinusoidal-dependent pressure associated with a rigid shoe and drum discussed in Section 2 nor the constant pressure associated with a deformable shoe and drum [4] may be used in this instance because the primary shoe is to pivot about the end of the adjusting link, which can only exert a force in the direction of the chord coincident with its centerline. Consequently, the lining pressure must be such that the primary shoe is in equilibrium when acted on by the pressure, the activating moment (due to the force from the brake cylinder), and the reaction of the adjusting link along its longitudinal axis.

From this last observation and from the geometry shown in Figure 13 we see that the radial and tangential forces must satisfy the relation

$$\tan\frac{\beta}{2} + \frac{F_r}{F_\theta} = 0 \tag{5-5}$$

where β is the angle at the center of the drum subtended by the adjusting link The magnitude of the link force is given by

$$F_l^2 = F_\theta^2 + F_r^2 \tag{5-6}$$

This link force and the activating moment both act on the secondary shoe, so that the force and moment equations of equilibrium for the secondary shoe become

$$F_{r_2} = -rw\int_{\phi_1}^{\phi_2} p \cos\phi \; d\phi + \mu rw\int_{\phi_2}^{\phi_1} p \sin\phi \; d\phi + F_l \sin\left(\phi_2 + \frac{\beta}{2}\right) \tag{5-7}$$

$$F_{\theta_2} = -rw\int_{\phi_1}^{\phi_2} p \sin\phi \; d\phi + \mu rw\int_{\phi_1}^{\phi_2} p \cos\phi \; d\phi + F_l \cos\left(\phi_2 + \frac{\beta}{2}\right) \tag{5-8}$$

where 2β is the angle subtended by the adjusting link. Next,

$$M_{a_2} = M_{p_2} + M_{f_2} - 2RF_l \sin\frac{\phi_2}{2} \sin\left(\frac{\phi_2}{2} + \frac{\beta}{2}\right) \tag{5-9}$$

where M_{p_2} and M_{f_2} are again given by equations (5.1) and (5.2) in terms of the pressure distribution on the secondary shoe. Torque for either shoe may be calculated from

$$T = \mu rw\int_{\phi_1}^{\phi_2} p \; d\phi \tag{5-10}$$

Even though these equations do not uniquely determine the pressure distribution over the brake lining, they are still of use because they allow the design engineer to compare the effects of different realistic pressure distribution and to design drums and shoes whose rigidity will induce particular pressure distributions over the primary and secondary shoes.

The first of the two pressure distributions considered is a synthesis of (1) the sinusoidal distribution associated with a nondeforming drum and shoe, generally associated with a lightly loaded brake, and (2) the force peaks that occur at the ends of load-bearing members in contact. The second of the two is a systhesis of (1) the constant distribution said to be associated with more heavily loaded brakes, and (2) the previously noted force peaks. Thus the pressure distributions will be represented either by

$$\frac{p}{p_0} = e^{-c_1(\psi/\phi_0)}\left|\cos\frac{\psi}{\phi_0}\pi\right|^{c_2} + c_3 \qquad \psi = \phi - \phi_1 \tag{5-11}$$

or by

$$\frac{p}{p_0} = e^{-c_1(\psi/\phi_0)}\left|\cos\frac{\psi}{\phi_0}\pi\right|^{c_2} + c_3 \sin(\psi + \phi_1) \tag{5-12}$$

for the primary shoes, where the peak pressure on each shoe occurs at the heel because its pivot cannot sustain a radial force in the outward direction. These relations produce the pressure distributions shown in Figures 14 and 15 for the values of c_1, c_2, and c_3 indicated. Similarly, peak pressure is assumed to occur at the toe of the secondary shoe, where it is subjected to the link force from the primary shoe. Since this shoe pivots at the anchor pin, it is assumed

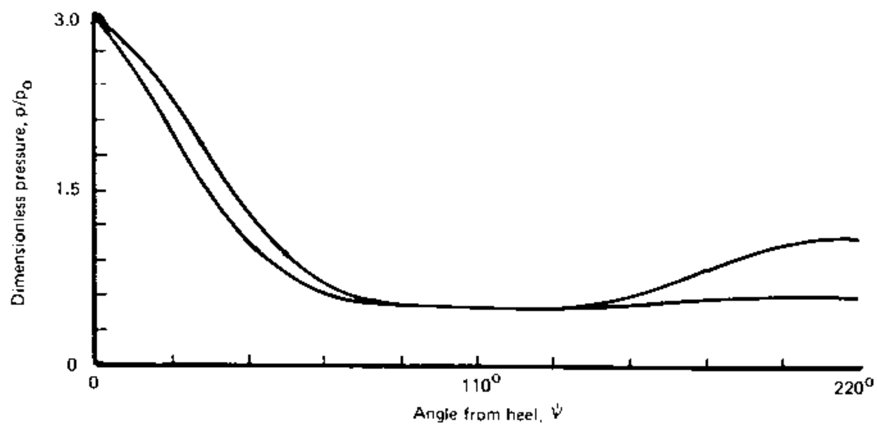

FIGURE 14 Primary pressure distributions.

that little or no increase in lining pressure is found at the heel of the secondary shoe. Thus the secondary shoe pressure distributions are represented by either

$$\frac{p}{p_0} = e^{-c_1(1 - \psi/\phi_0)} \left| \cos \frac{\psi}{\phi_0} \pi \right|^{c_2} + c_3 \tag{5-13}$$

or

$$\frac{p}{p_0} = e^{-c_1(1-\psi/\phi_0)} \left| \cos \frac{\psi}{\phi_0} \pi \right|^{c_2} + c_3 \sin(\psi + \phi_1) \tag{5-14}$$

which produce the distributions shown in Figures 16 and 17.

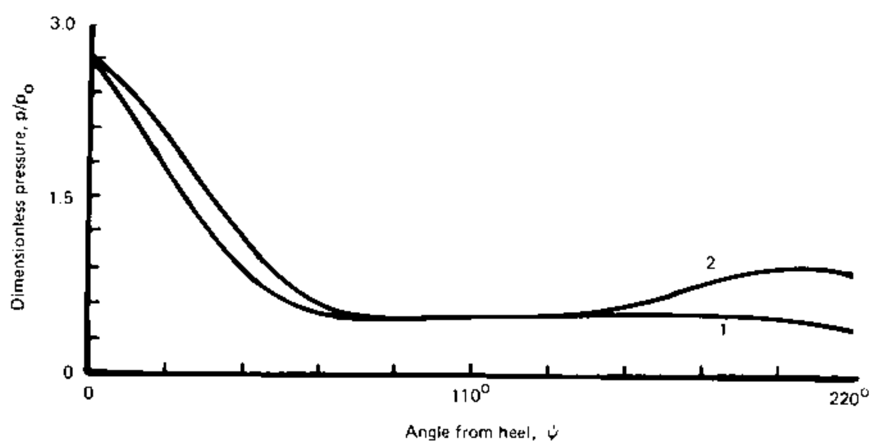

FIGURE 15 Primary pressure distributions.

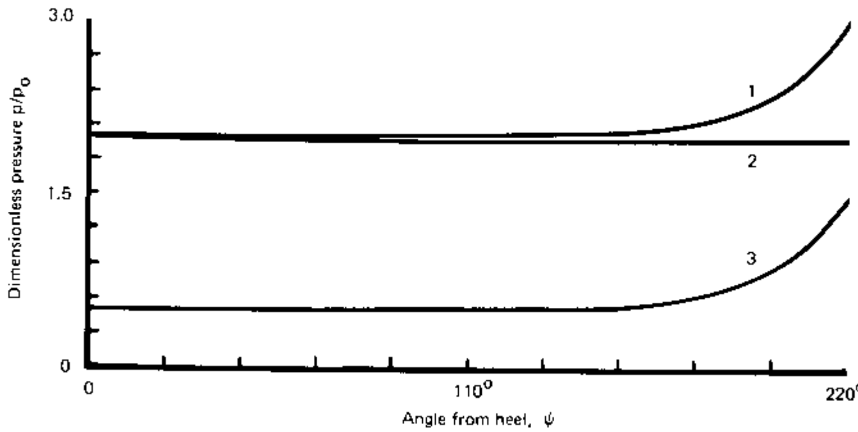

FIGURE 16 Secondary pressure distributions.

Since the secondary shoe is pivoted at the anchor pin, there are no restrictions on the direction of the resultant force and no particular mathematical restrictions on the pressure distribution itself other than that it not be infinite at any point along the shoe. The physical restrictions that these quantities be realistic motivated the use of pressure distributions similar to those on the primary shoes, based on the assumption that the shoe characteristics are similar, that the linings are very similar, if not identical, and that the force peak at the end of the shoe in contact with the link will be similar to

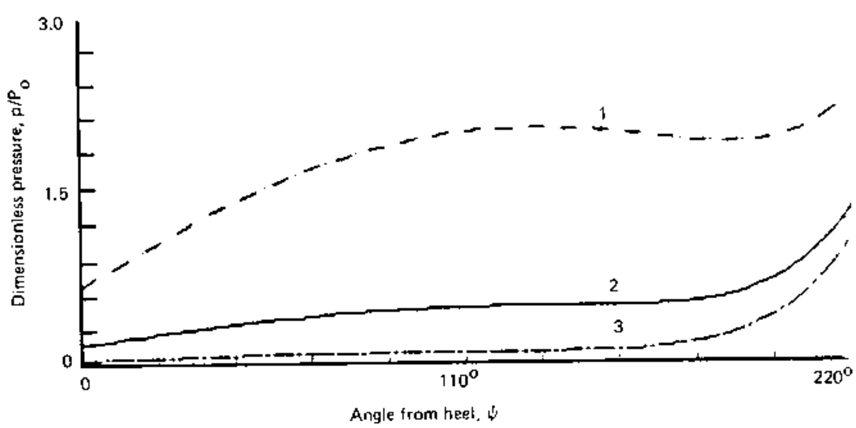

FIGURE 17 Secondary pressure distributions.

the force peak in the primary shoe at the other end of the link. Depending on the rigidity of the anchor pin and the rigidity of the brake shoe in the vicinity of the anchor pin, the force peak at this end of the lining may either be noticeably smaller than that at the free end of the primary shoe, or may vanish entirely.

The method of solution is to first solve for the unknown parameters in the expressions for the particular pressure distribution selected from either equations (5.11) or (5.12) on the primary shoe such that the condition

$$2\tan^{-1}\left(\frac{F_r}{F_\theta}\right) - \beta = 0 \tag{5-15}$$

is satisfied. Since this condition is independent of the lining pressure, that quantity may be found from the relation

$$M_1 = M_{p_1} + M_{f_1} \tag{5-16}$$

in which the external moment M_a is specified and where subscript 1 denotes the corresponding moment for the primary shoe.

With the maximum pressure on the primary shoe known, the pressure distribution over the primary shoe may be evaluated from equation (5-11) or (5-12), as appropriate, and the braking torque contributed by the primary shoe may then be calculated from equation (5-10). Link force may be found from equations (5-3), (5-4), and (5-6).

After selecting those values of c_1, c_2, and c_3 that provide a reasonable pressure distribution over the secondary shoe, the reference pressure may be found from equation (5-10) and the total braking torque becomes the sum of the torques contributed by the primary and secondary shoes.

VI. SINGLE-ANCHOR TWIN-SHOE DRUM BRAKE DESIGN EXAMPLES

Since it is the asymmetric term in the pressure distribution that is the major contributor to the control of the radial component of the force on the pivot point for a given coefficient of friction, satisfaction of equation (5-5) may be accomplished by adjusting the c_1 term in the pressure distribution. Once this is accomplished, the moment equilibrium conditions on the brake shoe may be satisfied by an appropriate choice of the pressure term, p_0. Equation (5-6) may then be evaluated to find the force transmitted to the primary shoe through the adjusting link. Straightforward calculation then yields the lining pressure for the secondary shoe and the torque contributed by both shoes.

Adjustment of constant c_1 may be carried out by finding the zero of the relation

$$\tan\frac{\beta}{2} + \frac{F_r}{F_\theta} = 0 \tag{6-1}$$

considered as a function of c_1. Location of a single zero in a given interval may be obtained using the bisection routine, such as in the TK Solver program.

It may appear that the search time may be reduced by restricting the search range for c_1 to a small neighborhood in the vicinity of the zeros found by displaying plots of equation (5-15) as a function of c_1 over an interval selected by the user for a range of values of μ, ϕ_1, and ϕ_2 suggested by the problem at hand. Plotting such a curve has proven to be unsatisfactory in practice because of the small intervals that are at times necessary to locate paired zeros. It may be faster to search for zeros by using a program that displays the integrands of F_r and F_t, their integrals, and their arctangents. This is because associating the asymmetry of the pressure distribution with the angle of the reaction at the adjusting link enables one quickly to see whether changes in the values of c_1 tend to bring the reaction into coincidence with the axis of the link. It also has the advantage of showing whether the constants chosen continue to represent adequately a physically reasonable pressure distribution.

A program for the numerical evaluation of the integrals involved in expressions (5-7) and (5-8) may easily be written using Simpson's rule. There appears to be only negligible improvement in accuracy obtained by dividing the interval into more than 50 segments.

The following four examples show the effect of changes in pressure distributions on brake performance and they also demonstrate the use of the method outlined. For this comparison all of the brake shoes subtend 120° at the center of the drum, they all have a 20° angle between the pivot and the heel of the shoe, and they all have an adjusting link which subtends 15° at the center of the drum. In addition, they are all subjected to an activating moment of 100 in.-lb and they all act on a drum having an inside diameter of 5.1 in. and a pivot at a radius of 4.2194 in. Results are summarized in Tables 2 and 3.

Example 6.1

Consider the dimensionless pressure distribution corresponding to curve 1 in Figure 14 and given by equation (5-11) with

$$c_1 = 3.15679 \qquad c_2 = 4.0 \qquad c_3 = 0.20$$

For this pressure distribution the maximum lining pressure at the heel is found to be 25.32 psi, the pressure at the toe of the shoe is 5.12 psi. the torque contribution from the primary shoe is 524.80 in.-lb, and the adjusting link is

TABLE 2 Lining Pressure and Shoe Braking Torque Associated with Primary Shoe Pressure Given by Equation (4-11) (Unit Width Shoe)

Shoe	Distribution number[a]	Heel pressure (psi)	Toe pressure (psi)	Link force (lb)	Torque (in.-lb)	Friction coefficient
P	1	25.320	5.320	1131.57	514.800	0.4
S	1	500.642	750.963	1131.57	2099.040	0.4
S	2	336.002	336.002	1131.57	2026.710	0.4
S	3	490.806	1472.418	1131.57	2310.270	0.4
P	2	25.320	9.390	908.55	338.200	0.3
S	1	314.318	417.477	908.55	988.383	0.3
S	2	321.610	321.610	908.55	969.967	0.3
S	3	294.334	883.001	908.55	1039.090	0.3

[a] *P* distributions are shown in Figure 14; *S* distributions are shown in Figure 16.

subjected to an axial force of 1131.57 lb. Upon imposing each of the three different pressure distributions shown in Figure 16 on the secondary shoe, it is found that although the maximum pressure distribution at the toe varies from about 336 to 1472 psi, the torque contribution from the secondary shoe only varies from 2027 to 2310 in.-lb.

Example 6.2

Reduction of the friction coefficient from 0.4 to 0.3 in equation (6.1) changes c_1 to 1.40460, and this change in turn modifies the pressure distribution acting over the primary shoe to that represented by curve 2 in Figure 14. The toe pressure remains unchanged, the central pressure drops, the heel pressure

TABLE 3 Lining Pressure and Shoe Braking Torque Associated with Primary Shoe Pressure Given by Equation (4-12) (Unit Width Shoe)

Shoe	Distribution number[a]	Heel pressure (psi)	Toe pressure (psi)	Link force (lb)	Torque (in.-lb)	Friction coefficient
P	1	21.140	3.380	1119.09	514.360	0.4
S	1	200.019	388.271	1119.09	2040.110	0.4
S	2	198.909	1544.466	1119.09	2277.790	0.4
S	3	170.460	6022.909	1119.09	3502.060	0.4
P	2	21.910	7.350	903.65	334.100	0.3
S	1	126.430	422.430	903.65	961.431	0.3
S	2	118.716	921.797	903.65	1019.600	0.3
S	3	92.300	2868.490	903.65	1245.890	0.3

[a] *P* distributions are shown in Figure 15; *S* distributions are shown in Figure 17.

increases to 9.39 psi, the link force (servo action) drops to 908.55 lb, and the torque contribution from the primary shoe falls to 338.20 in.-lb as a result of this change in the pressure distribution.

Secondary shoe pressures at the toe now range from 321.60 to 883.001 psi and the torque contributions from the secondary shoe now range from about 970 to 1039 in.-lb. Thus a 25% reduction in the friction coefficient has produced about a 58% reduction in the maximum torque capability of the secondary shoe, based on the 1039 in.-lb valve derived from distribution 3, Figure 16. Total torque capacity has dropped about 51%.

Example 6.3

Use of the primary distribution represented by curve 1 in Figure 15 and given by relation (5.15) with a friction coefficient of 0.4 leads to

$$c_1 = 3.45218 \qquad c_2 = 4.00 \qquad c_3 = 0.20$$

which produces a pressure distribution having lining pressures at the heel and toe of 21.14 and 3.38 psi, respectively, a torque contribution of 514.36 in.-lb, and a lining force (serve action) of 1119.09 lb. As shown in Figure 17, the pressure distributions on the secondary shoe produce maximum pressures ranging from about 388 to 6023 psi and torque contributions ranging from about 2040 to 3502 in.-lb. Maximum pressure and torque are both obtained from curve 3 in Figure 17.

Example 6.4

Reduction of the friction coefficient from 0.4 to 0.3 causes exponent c_1 to decrease to 1.51392, which corresponds to the dimensionless pressure distribution shown by curve 2 in Figure 15, wherein the heel and toe pressure become 7.35 and 21.91 psi, respectively. Braking torque from the primary shoe is calculated to be 334.100 in.-lb. and the link force is calculated to be 903.650 lb.

Secondary pressures at the toe of the lining for the pressure distributions shown in Figure 17 range from approximately 922 to 1246 in.-lb. In this case the 25% reduction in the coefficient of friction between drum and lining has produced almost a 61% reduction in the total braking torque.

Together these examples show that percentage changes in the torque capacity of the brake are a magnification of the percentage change in the friction coefficient. In large part this magnification appears to be due to the pressure maximum near the adjusting link which is necessary if the primary shoe is to be held in equilibrium by the link force and the lining pressure. Pressure distributions satisfying these equilibrium conditions may be of the form given by equations (5-11) and (5-12). Based on these pressure distributions, we have found that although the maximum pressure on the secondary shoe is strongly dependent on the width of the pressure maximum in the vicinity of the adjusting link, the magnitude of the braking torque contributed by the secondary shoe does not change quite as rapidly as the change in the lining pressure at the toe.

VII. ELECTRIC BRAKES

Common usage has associated the term electric brakes with friction brakes which are electrically activated, rather than with those brakes that rely upon electrical and magnetic forces rather than friction to provide the braking torque. Typical electric brakes are pictured in Figures 18 and 20. Both are single-anchor drum brakes that use the servo action associated with these brakes to obtain the required braking torque in response to an activating force indirectly related to the applied magnetic field.

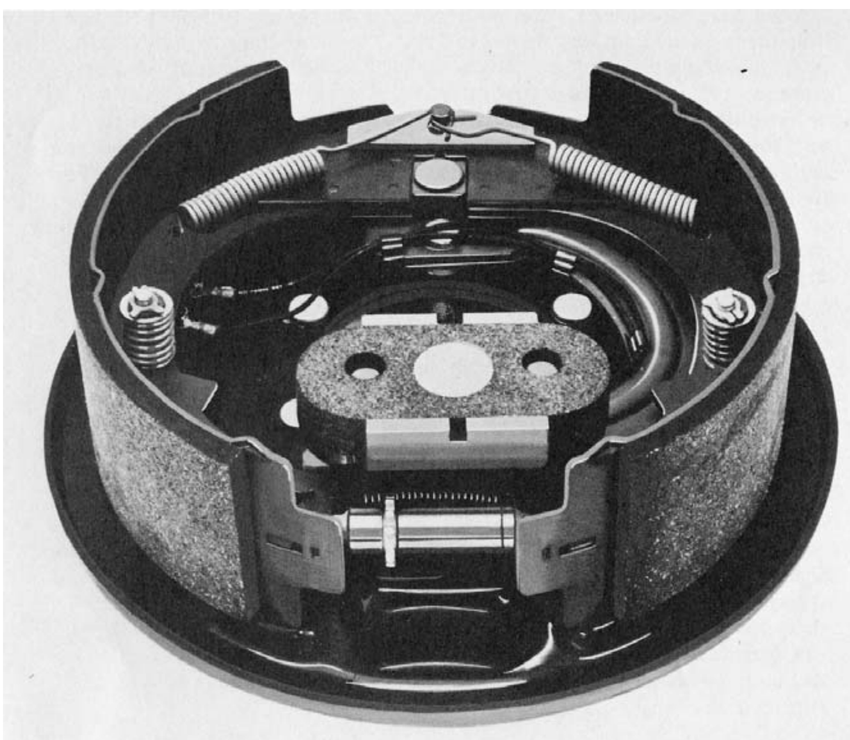

FIGURE 18 Electric drum brake activated by a cam attached to a magnet arm. (Courtesy of Warner Electric Brake & Clutch Co., South Beloit, IL.)

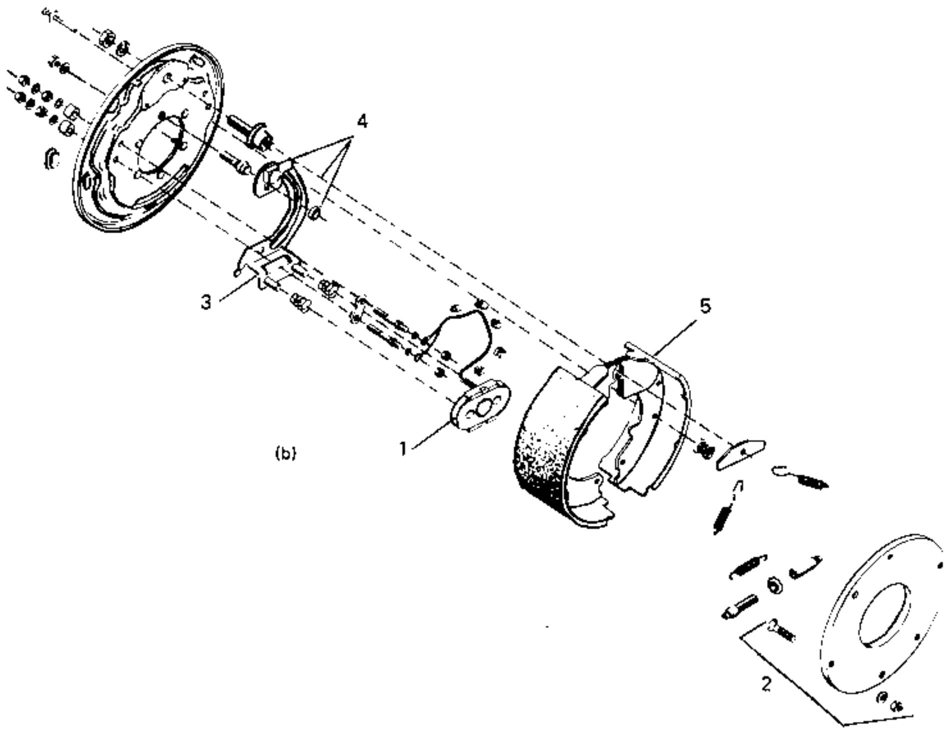

FIGURE 19 Exploded view of the components of the electric brake shown in Figure 18. (Courtesy of Warner Electric Brake & Clutch Co., South Beloit, IL.)

In the first type, shown in Figure 18, the small spot magnet 1 in Figure 19 is attracted to armature 2, which rotates with the drum. Friction between the spot magnet and the armature cause lever arm 3 to rotate and to actuate lever mechanism 4 to bring shoes 5 into contact with the drum. Depending upon the direction of rotation, one of these shoes will be the leading shoe, which by servo action will drive the trailing shoe against the drum.

Greater braking torque may be had from the model shown in Figure 20. In that design the annular electromagnet 1 in Figure 21 is attached to non-rotating backing plate by means of a pilot ring, which allows it to rotate slightly in the plane of the backing plate. When the electromagnet is energized it attracts armature 2, which rotates with the drum (not shown) but is allowed sufficient axial motion to contact the friction material on the face of the electromagnet. Friction between the electromagnet and the armature causes the electomagnet to rotate just enough to activate cam pair 3 (only one is shown)

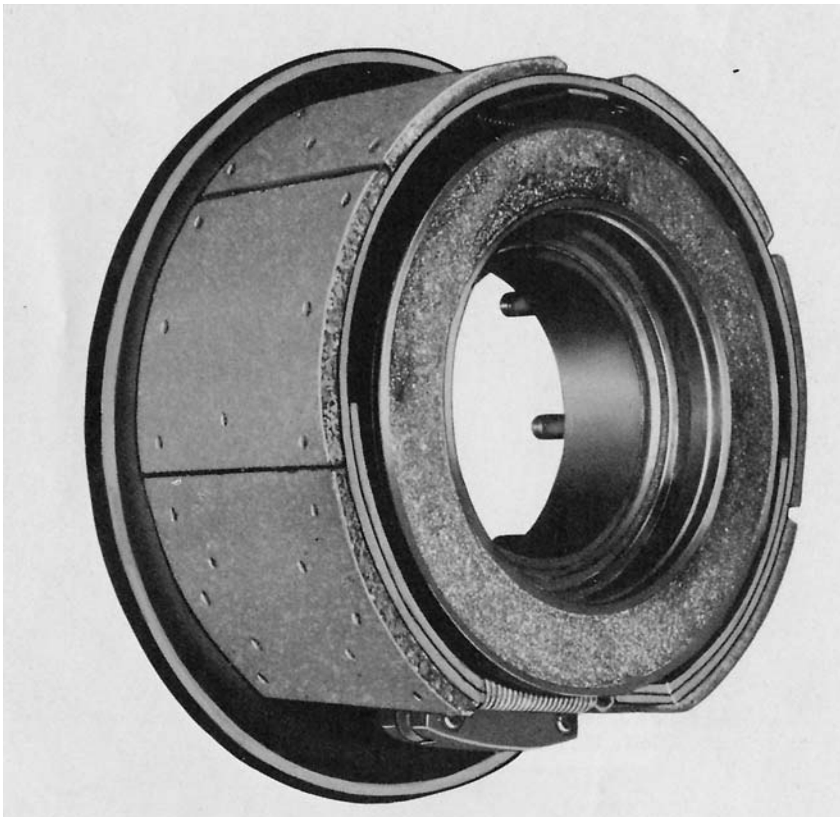

FIGURE 20 Electric drum brake activated by a cam and pin attached to the slightly rotating electromagnet. (Courtesy of Warner Electric Brake & Clutch Co., South Beloit, IL.)

and force shoes 4 against the drum. Again, servo action is relied upon to drive the trailing shoe against the drum so that together they provide a relatively large braking torque.

Simplified schematics of these two brakes which emphasize their means of operation are given in Figure 21.

These brakes were designed for use with highway trailers where a quick response time may be important. They have both fewer total parts and fewer exposed parts than either hydraulic or air brakes, but do not have as great a braking torque for a given size of drum and shoes.

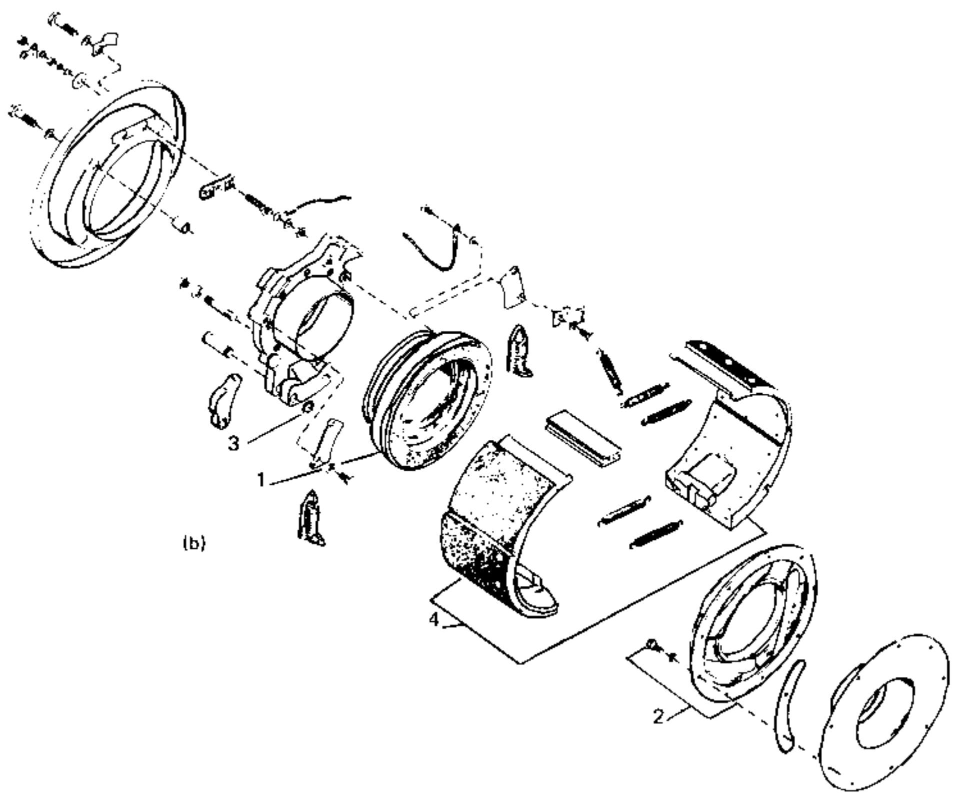

FIGURE 21 Exploded view of the components of the electric brake shown in Figure 20. (Courtesy of Warner Electric Brake & Clutch Co., South Beloit, IL.)

VIII. NOTATION

A	dummy variable (l)
B	dummy variable (l)
b	dummy variable (l^2)
b_a, b_b	dummy variables (mt^{-2})
c_1, c_2, c_3	pressure distribution coefficients (l)
F	force (mlt^{-2})
F_l	force along the axis of the adjusting link (mlt^{-2})
F_r	radial force (mlt^{-2})
F_θ	circumferential force (mlt^{-2})
k	effective spring constant of the lining (mt^{-2})
M_e	externally applied moment (ml^2t^{-2})

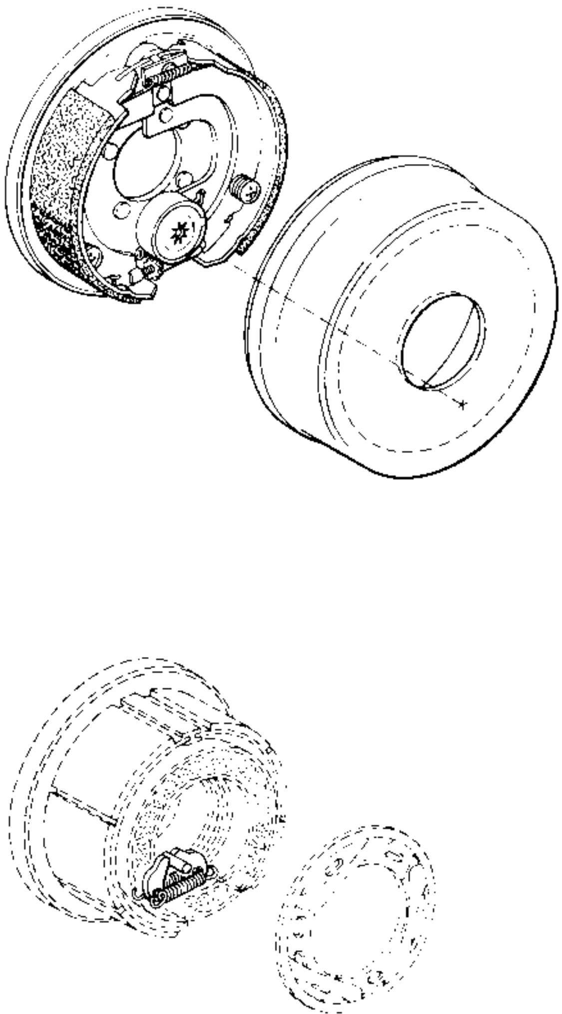

FIGURE 22 Schematic of brakes shown in Figures 18 and 20 to show method of operation. (Courtesy of Warner Electric Brake & Clutch Co., South Beloit, IL.)

M_f	moment on the shoe due to friction (ml^2t^{-2})
M_p	moment on the shoe due to lining pressure (ml^2t^{-2})
p	lining pressure ($ml^{-1}t^{-2}$)
p_0	reference pressure ($ml^{-1}t^{-2}$)
R	radius from drum center to shoe pivot point (l)
r	drum radius ($r = d/2$) (l)
T	torque (ml^2t^{-2})
T_a	torque contributed by primary shoe (ml^2t^{-2})
T_b	torque contributed by secondary shoe (ml^2t^{-2})
w	lining and shoe width (l)
β	half of the angle subtended by the adjusting link at the center of the drum (1)
$\delta\alpha$	angular motion of the shoe during braking (1)
μ	friction coefficient (1)
ϕ	angle subtended at the center of the drum (1)
ϕ_0	angle subtended by the lining at the center of the drum (1)
ψ	distribution parameter (1)

IX. FORMULA COLLECTION

A. Long Shoe–External and Internal

Angle subtended by the shoe:

$$\phi_0 = \phi_2 - \phi_1$$

Pressure:

$$p = \frac{p_{\max}}{(\sin\phi)_{\max}}$$

Torque:

$$T = \frac{\mu p_{\max} r w^2}{(\sin\phi)_{\max}}(\cos\phi_1 - \cos\phi_2)$$

Moment due to friction:

$$M_f = \frac{\mu p_{\max} r w}{4(\sin\phi)_{\max}}[R(\cos 2\phi_1 - \cos 2\phi_2) - 4r(\cos\phi_1 - \cos\phi_2)]$$

Moment due to pressure:

$$M_p = \frac{p_{\max} w r R}{4(\sin\phi)_{\max}}(2\phi_0 - \sin 2\phi_2 + \sin 2\phi_1)$$

External (activation) moment:

$$M_e = M_p \pm M_f \qquad \text{(see Table 1 to select proper sign)}$$

Radial force on a fixed anchor pin:

$$F_r = -r_w \int_{\phi_1}^{\phi_2} p \cos\phi \; d\phi + \mu r w \int_{\phi_1}^{\phi_2} p \sin\phi \; d\phi$$

Tangential force of a fixed anchor pin:

$$F_\theta = r_w \int_{\phi_1}^{\phi_2} p \sin\phi \; d\phi + \mu r w \int_{\phi_1}^{\phi_2} p \cos\phi \; d\phi$$

Figures 3–6 show the quantities involved in the foregoing formulas. Quantity ϕ_1 in the short-shoe formulas is identical to the same quantity defined for long shoes.

B. Short Shoe

Torque:

$$T = \mu p w r^2 \phi_0 = \mu r F$$

Pressure:

$$p = p_{\max}$$

Force:

$$F = p r w \phi_0$$

Moment due to friction:

$$M_f = \mu F (R \cos\phi_1 - r)$$

Moment due to pressure:

$$M_p = F R \sin\phi_1$$

REFERENCES

1. Burr, A. H. (1981). *Mechanical Analysis and Design*. New York: Elsevier.
2. Juvinal, R. C. (1983). *Fundamentals of Machine Component Design*. New York: Wiley.
3. Fazekas, G. A. G. (1958). Some basic properties of shoe brakes. *Journal of Applied Mechanics* 25:7–10.
4. Orthwein, W. C. (1985). Estimating torque and lining pressure for bendix type drum brakes. *SAE Paper 841234, SAE Transactions* 86:5.617–5.622.